

Unambiguous evidence for nearly isotropic s -wave gap in the bulk of optimally electron-doped $\text{Nd}_{1.85}\text{Ce}_{0.15}\text{CuO}_{4-y}$

Guo-meng Zhao^{1,2,*}

¹*Department of Physics and Astronomy, California State University, Los Angeles, CA 90032, USA*

²*Department of Physics, Faculty of Science, Ningbo University, Ningbo, P. R. China*

We address an important issue as to whether bulk-sensitive data of Raman scattering, optical conductivity, magnetic penetration depth, directional point-contact tunneling spectra, and nonmagnetic pair-breaking effect in optimally electron-doped $\text{Nd}_{1.85}\text{Ce}_{0.15}\text{CuO}_{4-y}$ support a nodeless s -wave or d -wave superconducting gap. We numerically calculate Raman intensities, directional point-contact tunneling spectra, and nonmagnetic pair-breaking effect in terms of both s -wave and d -wave gap symmetries. We find that all these bulk-sensitive data are in quantitative agreement with a nearly isotropic s -wave gap. The fact that T_c is nearly independent of the residual resistivity rules out any d -wave gap symmetry.

The gap symmetry of high-temperature cuprate superconductors has been a topic of intense debate for over twenty years. For hole-doped cuprates, bulk-sensitive experiments probing low-energy excitations in the superconducting state have consistently pointed towards the existence of line nodes in the gap function of hole-doped cuprates [1–4], which is consistent with either d -wave gap (having four line nodes) or extended s -wave gap (having eight line nodes). Other bulk-sensitive experiments on hole-doped cuprates [5, 6] can be quantitatively explained by extended s -wave gap [7]. In contrast, the issue as to whether there exist line nodes in the gap function of electron-doped (n -type) cuprates remains controversial. Phase and surface-sensitive experiments [8] provided evidence for pure d -wave order-parameter (OP) symmetry in optimally doped and overdoped n -type cuprates. Surface-sensitive angle-resolved photoemission spectroscopy (ARPES) [9, 10] showed a d -wave gap with a maximum gap size of about 2.5 meV. This gap size would imply a T_c of about 14 K at the surface, which is significantly lower than the bulk T_c of 26 K (Ref. [10]). Earlier magnetic penetration depth data [11] of optimally electron-doped cuprates with $T_c = 24$ K were shown to be consistent with nodeless s -wave gap symmetry. Later on, a T^2 dependence of the penetration depth at low temperatures was observed in $\text{Pr}_{1.85}\text{Ce}_{0.15}\text{CuO}_{4-y}$ ($T_c = 20$ K), which appears to support d -wave gap symmetry in the dirty limit [12]. But the same data can be quantitatively explained [7] in terms of a nodeless s -wave gap if one takes into account an extrinsic effect due to current-induced nucleation of vortex-antivortex pairs at defects. Extensive penetration depth data [13] of $\text{Pr}_{2-x}\text{Ce}_x\text{CuO}_{4-y}$ confirmed the nodeless gap symmetry at all the doping levels except for a deeply underdoped $\text{Pr}_{1.885}\text{Ce}_{0.115}\text{CuO}_{4-y}$ sample with $T_c = 12$ K. Point-contact tunneling spectra [14–18] also showed no zero-bias conductance peak (ZBCP) at all the doping levels except for a deeply underdoped $\text{Pr}_{1.87}\text{Ce}_{0.13}\text{CuO}_{4-y}$ with $T_c = 12$ K. Therefore, the penetration depth and point-contact tunneling spectra consistently suggest that the gap symmetry in deeply underdoped samples should

be d -wave and change to a nodeless s -wave when the doping level is above a critical value. This scenario can naturally explain the d -wave gap symmetry inferred from surface-sensitive experiments if surfaces or interfaces are deeply underdoped. Experiments on hole-doped cuprates [19, 20] indeed show that surfaces and interfaces are significantly underdoped.

Here we focus on optimally electron-doped $\text{Nd}_{1.85}\text{Ce}_{0.15}\text{CuO}_{4-y}$ (NCCO) to unambiguously address this important issue as to whether bulk-sensitive data of Raman scattering, optical conductivity, magnetic penetration depth, directional point-contact tunneling spectra, and nonmagnetic pair-breaking effect support a nodeless s -wave gap. We numerically calculate Raman intensities, directional point-contact tunneling spectra, and nonmagnetic pair-breaking effect in terms of both s -wave and d -wave gap symmetries. We find that all these bulk-sensitive data are in quantitative agreement with a nearly isotropic s -wave gap. The fact that T_c is nearly independent of the residual resistivity rules out any d -wave gap symmetry.

Bulk-sensitive Raman scattering has been proved to be a very powerful tool to study the anisotropy of the superconducting energy gap. Experiments carried out with different polarization orientations pick up the contributions to the light scattering on different parts of the Fermi surface. The B_{1g} spectra provide information on the light scattering primarily in the neighborhood of the k_x and k_y axes while B_{2g} spectra probe mainly along the diagonals, where $(k_x, k_y) = \vec{k}$ is the in-plane wave vector of electrons. The electronic Raman intensity is proportional to the imaginary part of Raman susceptibility $\chi_{\gamma\gamma}(\vec{q}, \omega)$ in the limit of \vec{q} approaching 0. At zero temperature, the imaginary part of $\chi_{\gamma\gamma}(\omega)$ is given by [21]

$$\text{Im}\chi_{\gamma\gamma}(\omega) = \sum_{\vec{k}} \frac{\gamma^2(\vec{k})\Delta^2(\vec{k})}{E^2(\vec{k})} \left[\frac{\Gamma}{(\omega - 2E(\vec{k}))^2 + \Gamma^2} - \frac{\Gamma}{(\omega + 2E(\vec{k}))^2 + \Gamma^2} \right], \quad (1)$$

where $\Delta(\vec{k})$ is the momentum-dependent superconduct-

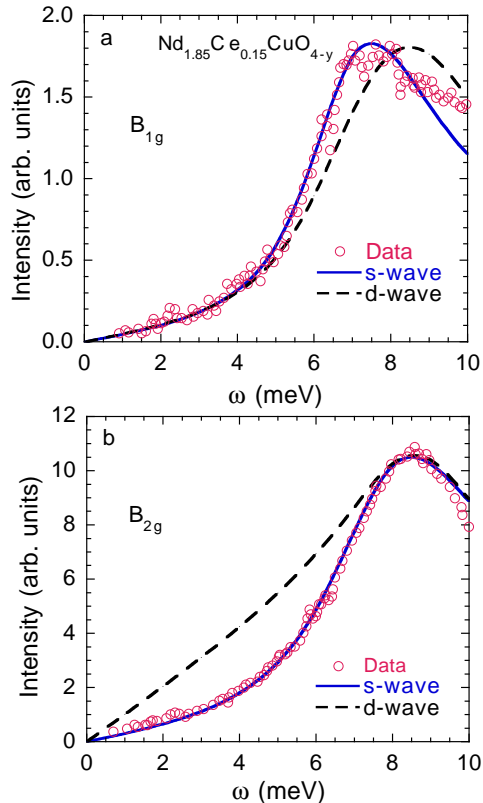


FIG. 1: Raman intensities at 8 K for $\text{Nd}_{1.85}\text{Ce}_{0.15}\text{CuO}_{4-y}$ ($T_c = 22 \pm 1$ K) in the B_{1g} (Fig. 1a) and B_{2g} (Fig. 1b) symmetries. The data are digitized from Ref. [24]. The solid lines are numerically calculated curves in terms of an anisotropic s -wave gap function: $\Delta = 3.59(1 - 0.11 \cos 4\theta)$ meV with $\Gamma = 1.4$ meV for the B_{1g} channel and $\Gamma = 1.9$ meV for the B_{2g} channel; the dashed lines are the numerically calculated curve in terms of a non-monotonic d -wave gap function: $\Delta = 3.25(1.43 \cos 2\theta - 0.43 \cos 6\theta)$ meV with $\Gamma = 1.6$ meV for both channels.

ing energy gap, $E(\vec{k}) = \sqrt{\Delta^2(\vec{k}) + \epsilon^2(\vec{k})}$, Γ is the parameter associated with the life-time broadening of the quasiparticles, $\epsilon(\vec{k})$ is the band-dispersion relation, and $\gamma(\vec{k})$ is the Raman vertex which is proportional to $\cos k_x a - \cos k_y a$ for B_{1g} symmetry and to $\sin k_x a \sin k_y a$ for B_{2g} symmetry (where a is the lattice constant) [22]. By fitting ARPES data, the band-dispersion relation $\epsilon(\vec{k})$ (in units of meV) for $\text{Nd}_{1.85}\text{Ce}_{0.15}\text{CuO}_{4-y}$ was found to be [23]

$$\begin{aligned} \epsilon(\vec{k}) = & -460(\cos k_x a + \cos k_y a) + 220 \cos k_x a \cos k_y a \\ & -70(\cos 2k_x a + \cos 2k_y a) + 60(\cos 2k_x a \cos k_y a \\ & + \cos k_x a \cos 2k_y a) - 27 \quad (2) \end{aligned}$$

Figure 1 shows B_{1g} and B_{2g} Raman intensities at 8 K for $\text{Nd}_{1.85}\text{Ce}_{0.15}\text{CuO}_{4-y}$ with $T_c = 22 \pm 1$ K. The data are digitized from Ref. [24]. The solid lines are numerically calculated curves using Eqs. 1 and 2, $\Gamma = 1.4$ meV for the

B_{1g} channel, $\Gamma = 1.9$ meV for the B_{2g} channel, and $\Delta = 3.59(1 - 0.11 \cos 4\theta)$ meV, where θ is measured from the Cu-O bonding direction. It is remarkable that the calculated curves match very well with the experimental data. Furthermore, the minimum value Δ_{min} of this gap function is 3.2 meV, which is close to that (3 meV) deduced from the magnetic penetration depth [11]. The optical reflectance of a similar $\text{Nd}_{1.85}\text{Ce}_{0.15}\text{CuO}_{4-y}$ crystal with $T_c = 23$ K also shows a minimum gap of about 3.1 meV at 10 K (Ref. [25]). For comparison, we also numerically calculate Raman intensities in terms of a non-monotonic d -wave gap function: $\Delta = 3.25(1.43 \cos 2\theta - 0.43 \cos 6\theta)$ meV (dashed lines). This gap size, which is a factor of 1.7 larger than that extracted from ARPES [10], matches the peak position of the B_{2g} Raman spectrum. It is apparent that the B_{2g} Raman spectrum is inconsistent with any d -wave gap function with nodes along the Cu-Cu directions.

Further evidence for the nodeless s -wave gap symmetry comes from the directional point-contact tunneling spectra of optimally doped $\text{Nd}_{1.85}\text{Ce}_{0.15}\text{CuO}_{4-y}$ ($T_c = 25$ K). It was argued that single-particle tunneling experiments along the CuO_2 planes can probe the bulk electronic density of states since the mean free path is far larger than the thickness of the possibly degraded surface layer [26]. Figure 2 shows the in-plane point-contact tunneling spectra of $\text{Nd}_{1.85}\text{Ce}_{0.15}\text{CuO}_{4-y}$ measured along (100) direction (Fig. 2a) and (110) direction (Fig. 2b), respectively. The data are digitized from Ref. [17]. One can calculate point-contact tunneling spectra using the Blonder-Tinkham-Klapwijk (BTK) theory [27]. In this model, two parameters are introduced to describe the effective potential barrier (Z) and the superconducting energy gap Δ . As a supplement, the quasiparticle energy E is replaced by $E - i\Gamma$, where Γ is the broadening parameter characterizing the finite lifetime of the quasiparticles. Based on the BTK theory, Shan *et al.* calculate the tunneling conductance in terms of the isotropic s -wave gap function [17]. The agreement between the calculated curve and data is excellent for each tunneling spectrum. However, the gap sizes that used to fit the tunneling spectra along the (100) and (110) directions are slightly different. This implies that the gap is not isotropic.

For the extended anisotropic BTK model [28], another parameter α is introduced to distinguish between different tunneling directions. In Fig. 2, we compare the tunneling spectra with the calculated curves based on the extended anisotropic BTK model and an anisotropic s -wave gap function: $\Delta = 3.52(1 - 0.17 \cos 4\theta)$ meV. The solid line in Fig. 2a is the numerically calculated curve using $Z = 2.8$, $\Gamma = 0.86$ meV, and $\alpha = 0$ and the solid line in Fig. 2b is the calculated curve using $Z = 3.0$, $\Gamma = 0.65$ meV, and $\alpha = \pi/4$. It is apparent that the calculated curves are in excellent agreement with the data.

In Figure 3, we compare the tunneling spectra with the calculated curves in terms of a nonmonotonic d -wave

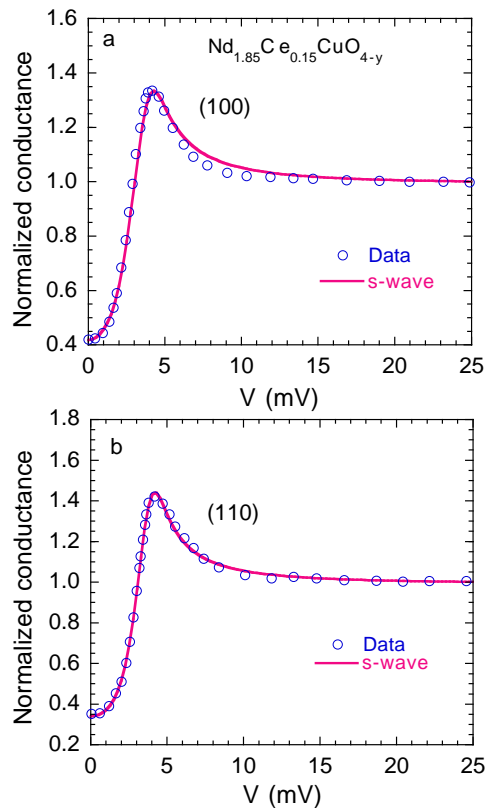


FIG. 2: In-plane point-contact tunneling spectra of $\text{Nd}_{1.85}\text{Ce}_{0.15}\text{CuO}_{4-y}$ ($T_c = 25$ K) measured along (100) direction (Fig. 2a) and (110) direction (Fig. 2b), respectively. The data are digitized from Ref. [17]. The solid line in Fig. 2a is the numerically calculated curve using $Z = 2.8$, $\Gamma = 0.86$ meV, and $\alpha = 0$ and the solid line in Fig. 2b is the calculated curve using $Z = 3.0$, $\Gamma = 0.65$ meV, and $\alpha = \pi/4$. The gap function used in the calculations is $\Delta = 3.52(1 - 0.17 \cos 4\theta)$ meV.

gap function: $\Delta = 3.0(1.43 \cos 2\theta - 0.43 \cos 6\theta)$ meV. The solid lines are the numerically calculated curves using $Z = 3.0$, $\Gamma = 0.65$ meV, $\alpha = 0$ for the spectrum along (100) direction, and $\alpha = \pi/4$ for the spectrum along (110) direction. One can see that, for the tunneling spectrum along (100) direction, the calculated curve coincides with the data at high bias voltages but significant deviations occur at low bias voltages. For tunneling spectrum along (110) direction, ZBCP is clearly seen in the calculated curve, in sharp contrast to the data. Therefore, the tunneling spectra cannot be explained by d -wave gap symmetry.

Finally, the most powerful way to distinguish between any d -wave and anisotropic s -wave gap symmetries is to study the response of a superconductor to nonmagnetic impurities or disorder. The nonmagnetic impurity pair-breaking effect is both bulk- and phase-sensitive. This is because the rate of T_c suppression by nonmagnetic im-

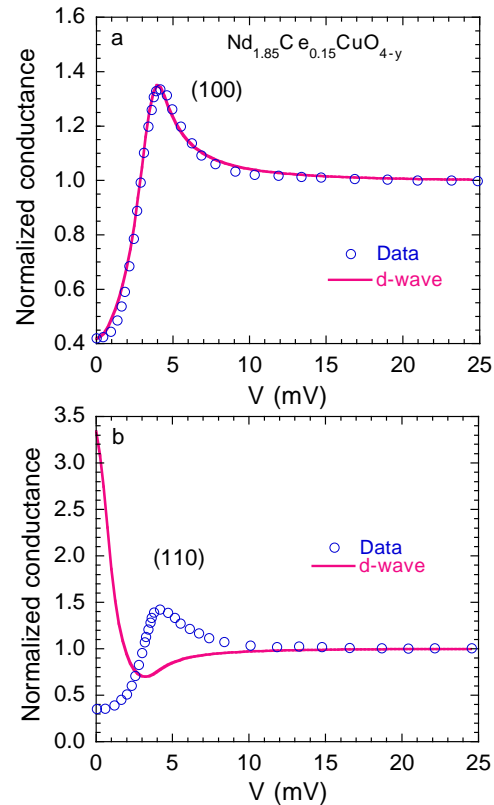


FIG. 3: Comparison of the tunneling spectra of NCCO with the calculated curves based on a nonmonotonic d -wave gap function: $\Delta = 3.0(1.43 \cos 2\theta - 0.43 \cos 6\theta)$ meV. The solid lines are the numerically calculated curve using $Z = 3.0$, $\Gamma = 0.65$ meV, and $\alpha = 0$ for the spectrum along (100) direction and $\alpha = \pi/4$ for the spectrum along (110) direction, respectively.

purities or defects in a two-dimensional superconductor [29] is determined by the value of the Fermi surface (FS) average $\langle \Delta(\vec{k}) \rangle_{FS}$, which depends sensitively on the phase of the gap function. More specifically, the rate is proportional to a parameter $\chi = 1 - (\langle \Delta(\vec{k}) \rangle_{FS})^2 / \langle \Delta^2(\vec{k}) \rangle_{FS}$. It is clear that $\chi = 0$ for isotropic s -wave superconductors while $\chi = 1$ for d -wave and g -wave superconductors. For the anisotropic s -wave gap: $\Delta = 3.59(1 - 0.11 \cos 4\theta)$ meV, $\chi = 0.006$. An equation to describe the pair-breaking effect by nonmagnetic impurities (or defects) is given by [29]

$$\ln \frac{T_{c0}}{T_c} = \chi \left[\Psi\left(\frac{1}{2} + \frac{0.122(\hbar\Omega_p^*)^2 \rho_r}{T_c}\right) - \Psi\left(\frac{1}{2}\right) \right], \quad (3)$$

where $\hbar\Omega_p^*$ is the renormalized plasma energy [29, 30] in units of eV, ρ_r is the residual resistivity in units of $\mu\Omega\text{cm}$, and Ψ is the digamma function. The renormalized plasma energy can be independently determined from optical conductivity. Optical data of $\text{Pr}_{1.85}\text{Ce}_{0.15}\text{CuO}_{4-y}$ indicate $\hbar\Omega_p^* = 1.64$ eV (Ref. [31]). We will use this value

of $\hbar\Omega_p^*$ to calculate T_c as a function of the residual resistivity in terms of both d -wave and an anisotropic s -wave gap function inferred from the Raman spectra above.

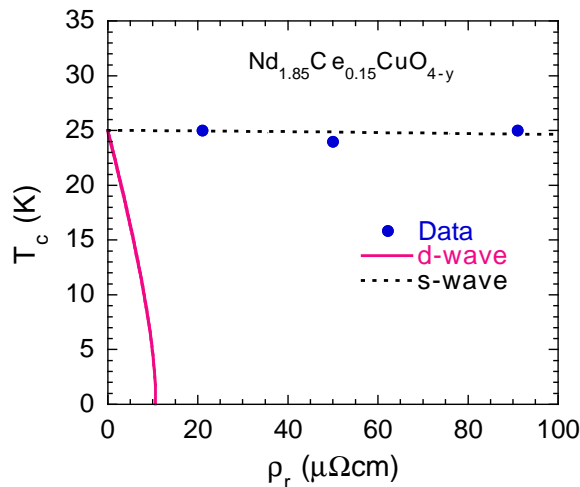


FIG. 4: T_c as a function of residual resistivity in optimally doped $\text{Nd}_{1.85}\text{Ce}_{0.15}\text{CuO}_{4-y}$. The data are from Refs. [11, 17, 32]. The solid line is numerically calculated curve in terms of any d -wave gap and the dotted line is the calculated curve for an s -wave gap function proportional to $(1 - 0.11 \cos 4\theta)$.

Figure 4 shows T_c as a function of residual resistivity in optimally doped $\text{Nd}_{1.85}\text{Ce}_{0.15}\text{CuO}_{4-y}$. The data are from Refs. [11, 17, 32]. The solid line is the numerically calculated curve in terms of any d -wave gap and the dotted line is the calculated curve for an s -wave gap function proportional to $(1 - 0.11 \cos 4\theta)$. For the d -wave gap symmetry, the parameter-free calculation (solid line) shows that T_c will be suppressed to zero at a very small residual resistivity of $10.7 \mu\Omega\text{cm}$ while the measured T_c is nearly independent of the residual resistivity. For the s -wave gap proportional to $(1 - 0.11 \cos 4\theta)$ or to $(1 - 0.17 \cos 4\theta)$, the calculated T_c is nearly independent of the residual resistivity, in agreement with the data. Therefore, the data in Fig. 4 rule out any d -wave gap symmetry and unambiguously point towards nodeless s -wave gap symmetry.

In summary, the bulk-sensitive data of Raman scattering, optical conductivity, magnetic penetration depth, directional point-contact tunneling spectra, and nonmagnetic pair-breaking effect in optimally electron-doped $\text{Nd}_{1.85}\text{Ce}_{0.15}\text{CuO}_{4-y}$ unambiguously support a nearly isotropic s -wave gap. The s -wave gap symmetry is consistent with the earlier [33] and recent [34] conclusion that high-temperature superconductivity in electron-doped cuprates is mainly caused by electron-phonon coupling.

*Correspondence should be addressed to gzhao2@calstatela.edu

-
- [1] W. N. Hardy *et al.*, Phys. Rev. Lett. **70**, 3999 (1993).
 - [2] T. Jacobs *et al.*, Phys. Rev. Lett. **75**, 4516 (1995).
 - [3] S.-F. Lee *et al.*, Phys. Rev. Lett. **77**, 735 (1996).
 - [4] M. Chiao *et al.*, Phys. Rev. B **62**, 3554 (2000).
 - [5] A. Bhattacharya *et al.*, Phys. Rev. Lett. **82**, 3132 (1999).
 - [6] Q. Li *et al.*, Phys. Rev. Lett. **83**, 4160 (1999). This phase-sensitive experiment is considered to be bulk-sensitive because the measured product of the critical current I_c and the junction resistance R_N is in quantitative agreement with the expected bulk value [7].
 - [7] G. M. Zhao, Phys. Rev. B **64**, 024503 (2001).
 - [8] C. C. Tsuei, and J. R. Kirtley, Phys. Rev. Lett. **85**, 182 (2000); A. D. Darminto *et al.*, Phys. Rev. Lett. **94**, 167001 (2005). These phase-sensitive experiments are surface-sensitive because the inferred magnitude of the order parameter from the measured critical current I_c and junction resistance R_N is about two orders of magnitude too smaller than the expected bulk value.
 - [9] N. P. Armitage *et al.*, Phys. Rev. Lett. **86**, 1126 (2001).
 - [10] H. Matsui *et al.*, Phys. Rev. Lett. **95**, 017003 (2005).
 - [11] L. Alff *et al.*, Phys. Rev. Lett. **83**, 2644 (1999).
 - [12] R. Prozorov, R. W. Giannetta, P. Fournier, and R. L. Greene, Phys. Rev. Lett. **85**, 03700 (2000).
 - [13] Mun-Seog Kim *et al.*, Phys. Rev. Lett. **91**, 087001 (2002).
 - [14] S. Kashiwaya *et al.*, Phys. Rev. B **57**, 8680, (1998).
 - [15] Amlan Biswas *et al.*, Phys. Rev. Lett. **88**, 207004 (2002).
 - [16] M. M. Qazilbash *et al.*, Phys. Rev. B **68**, 024502 (2003).
 - [17] L. Shan *et al.*, Phys. Rev. B **72**, 144506 (2005).
 - [18] L. Shan *et al.*, Phys. Rev. B **77**, 014526 (2008).
 - [19] J. Betouras and R. Joynt, Physica C **250**, 256 (1995).
 - [20] J. Mannhart and H. Hilgenkamp, Physica C **317-318**, 383 (1999).
 - [21] D. Branch, and J. P. Carbotte, Phys. Rev. B. **52**, 603 (1995).
 - [22] T. P. Devereaux, A. Virosztek, and A. Zawadowski, Phys. Rev. B. **54**, 12523 (1996).
 - [23] R. S. Markiewicz *et al.*, Phys. Rev. B. **72**, 054519 (2005).
 - [24] G. Blumberg *et al.*, Phys. Rev. Lett. **88**, 107002 (2002).
 - [25] C. C. Homes, B. P. Clayman, J. L. Peng, and R. L. Greene, Phys. Rev. B **56**, 5525 (1997).
 - [26] Ya. G. Ponomarev *et al.*, Physica C **243**, 167 (1995).
 - [27] G. E. Blonder, M. Tinkham, and T. M. Klapwijk, Phys. Rev. B **25**, 4515 (1982).
 - [28] Y. Tanaka and S. Kashiwaya, Phys. Rev. Lett. **74**, 3451 (1995).
 - [29] L. A. Openov, Phys. Rev. B **58**, 9468 (1998).
 - [30] R. J. Radtke, K. Levin, H.-B. Schutter, M. R. Norman, Phys. Rev. B **48**, 653 (1993).
 - [31] C. C. Homes *et al.*, Phys. Rev. B **74**, 214515 (2006).
 - [32] Y. Onose, Y. Taguchi, K. Ishizaka, and Y. Tokura, Phys. Rev. B **69**, 024504 (2004).
 - [33] Q. Huang *et al.*, Nature (London) **347**, 369 (1990).
 - [34] G. M. Zhao, Phys. Rev. Lett. **103**, 236403 (2009).